NATIONAL AERONAUTICS AND SPACE ADMINISTRATION

Technical Memorandum 33-509

Development and Testing of the Infrared Interferometer Spectrometer for the Mariner Mars 1971 Spacecraft

JET PROPULSION LABORATORY
CALIFORNIA INSTITUTE OF TECHNOLOGY
PASADENA, CALIFORNIA

December 1, 1971

NATIONAL AERONAUTICS AND SPACE ADMINISTRATION

Technical Memorandum 33-509

Development and Testing of the Infrared Interferometer Spectrometer for the Mariner Mars 1971 Spacecraft

JET PROPULSION LABORATORY
CALIFORNIA INSTITUTE OF TECHNOLOGY
PASADENA, CALIFORNIA

December 1, 1971

PREFACE

The work described in this report was performed by the technical divisions of the Jet Propulsion Laboratory, under the cognizance of the Mariner Mars 1971 Project.

ACKNOWLEDGMENT

The information documented in this report was compiled by R. H. Hanel and B. Schlachman (Goddard Space Flight Center); D. Vanous and D. Rogers (Texas Instruments, Inc.), and J. Taylor (Jet Propulsion Laboratory) using contributions from the following people:

D. Bywaters (TI)	Thermal design
E. Breihan (TI)	CsI beamsplitter
F. Chapman, M. Rhodes, and J. Sackett (TI)	Electronic design and testing
H. Eyerly and T. Burke (JPL)	Interface/system testing
W. Miller (GSFC)	Bit error detection and correction subsystem

CONTENTS

FIGURES (contd)

ABSTRACT

This report covers the design, development and testing of the infrared interferometer spectrometer with emphasis placed on the unique features of the Mariner instrument as compared to previous IRIS instruments flown on the Nimbus meteorological research satellites. The interferometer functions in the spectral range from 200 cm^{-1} (50 μ) to 1600 cm^{-1} (6.3 μ) with an apodized spectral resolution equivalent to 2.4 cm^{-1}. A noise equivalent radiance of 0.5×10^{-7} W cm^{-2} $ster^{-1}/cm^{-1}$ has been achieved. Major improvements that were implemented included the cesium iodide beamsplitter and electronic features to suppress the effect of vibration on the Michelson mirror motion and digital filtering through the summation of increased sampling of the infrared signal. A bit error detection and correction scheme was also implemented in order to recover the science data with a higher level of confidence over the telecommunication link.

I. INTRODUCTION

The primary purpose of the Mariner Mars 1971 infrared spectroscopy experiment is to determine values of atmospheric parameters and information pertinent to the solid surface of Mars. Among the atmospheric parameters sought are (1) CO_2 pressure at the surface, (2) vertical temperature profile, (3) total amount of water vapor in an atmospheric column and possibly its vertical distribution, and (4) the concentration or upper limit of minor gaseous constituents. Parameters related to the surface are temperature, mineral composition, and data on the physical state of the surface, such as discrimination between solid rock, gravel and fine sand. All of these parameters can be derived by interpretation of thermal emission spectra, which will be observed from the orbiter as a function of time and location on the planet. It is hoped that a much improved model of atmospheric and surface conditions of Mars may be constructed and that Martian meteorology, geology and possibly biology may experience substantial advances.

The Mars infrared interferometer spectrometer (IRIS-M) optical module with the thermal blanket installed is shown in Fig. 1 prior to its installation on the scan platform. Also shown are the bay electronics modules. The IRIS-M covers the spectral range from 200 cm^{-1} (50 μ) to 1600 cm^{-1} (6.3 μ) with a spectral resolution equivalent to 2.4 cm^{-1}. A noise equivalent radiance of 0.5×10^{-7} W cm^{-2} $ster^{-1}/cm^{-1}$ has been achieved during system thermal vacuum tests.

The Mariner interferometer, which was designed, fabricated and tested by Texas Instruments, Inc., under the direction of NASA/Goddard Space Flight Center, is similar to the interferometer flown on the meteorological research satellites Nimbus 3 (IRIS-B) and Nimbus 4 (IRIS-D) in 1969 and 1970, respectively (Refs. 1 and 2). The IRIS-M reproduces many of the desirable design features from IRIS-D. Therefore, to avoid

repetition in this report, emphasis will be placed on the unique features of IRIS-M, with particular regard to the cesium iodide (CsI) beamsplitter (Ref. 3). The extension of the spectral range from 400 to 200 cm^{-1} made possible with the CsI beamsplitter is significant to the water vapor investigation since the spectral range between 200 and 400 cm^{-1} contains several strong rotational water vapor lines. The increased spectral resolution achieved on IRIS-M (18% greater than IRIS-D) is particularly important in the search for minor constituents. Several major changes were required to accommodate the increase in performance and to adapt to the Mariner spacecraft environment. The first class of changes includes (1) a photomultiplier in lieu of a silicon detector for the neon reference interferometer, (2) a delay line in the data sampling signal to improve the immunity of the instrument against external vibration, (3) an increase in the number of bits in each science data word, and (4) an error detection and correction system to reduce the effect of bit errors in the data telecommunication link. The second class of changes, dictated by the necessity of adapting to the Mariner spacecraft, includes modifications in the mechanical configuration, power system, optics thermal controller, blackbody temperature controller and data handling circuitry. The start position control circuit for the Michelson mirror, that operated very successfully on IRIS-D, was deleted on IRIS-M early in the program when it appeared that the weight and power limitations would be difficult to meet. The deletion had no effect on the spectral resolution at the operational temperatures of 250°K, since at this temperature the zero path distance word for IRIS-M was adjusted approximately in the center of the interferogram.

II. DESIGN AND DEVELOPMENT

In general, the overall features of the Mariner interferometer are similar to those of the earlier models. The most important design parameters and characteristics of the Nimbus and Mariner instruments are compared in Table 1. Major changes were made in the following areas for increased performance and compatibility with the Mariner spacecraft:

Electrical

- Power supplies
- Clock frequencies
- Commands
- Data format
- Distribution of subassemblies

Mechanical

- Support structure
- Optical housings
- Viewports
- Bay chassis

Thermal

- Temperature range
- Cruise/orbit modes
- Scan platform motion
- Thermal blanket
- Heater power

Operational Vibration

- Delay line (neon sampling delay)
- Summation circuit

Launch Vibration

- Shock mounts
- Beamsplitter mount
- Fixed mirror mount
- Michelson motor mount

Bit Error Rate, Telecommunication Link

Error detection and correction

Spectral Resolution and Bandwidth

Photomultiplier tube

Increased Michelson mirror travel

CsI window and beamsplitter

A. Optical/Mechanical Development

1. Beamsplitter. The CsI beamsplitter is probably the most significant optical improvement made to IRIS-M. The CsI development started with IRIS-D, but was not completed in time for the Nimbus 4 launch.

The CsI beamsplitter made it possible for IRIS-M to record the infrared emission spectrum between 200 and 1600 cm^{-1}. The beamsplitter mount (Fig. 2) is similar in configuration to the KBr beamsplitters for the interferometers flown on Nimbus. The substrates, cut from a single crystal CsI, are 0.95 cm thick and 8.2 cm in diameter, with each surface polished flat to at least 0.5×10^{-4} cm. Prior to the deposition of the optical coatings the substrates are dipped into a solution of photoresist and acetone which serves as a protective coating against humidity during the handling of the substrates. The infrared coating is a 10-layer configuration consisting of alternate layers of lead fluoride, KRS-5, and germanium. The visible section (used for the reference interferometer) is located in the center of the beamsplitter substrate and has a coating of seven layers consisting of layers of zinc sulfide and thorium oxyfluoride. Aluminum type 6061-T651 is used for the mounting rings to which the substrates are bonded with General Electric Co. RTV 630 silicon rubber. The two halves of the mounting rings are also bonded together with RTV 630. The complete assembly is subjected to flight acceptance tests (vibration and temperature cycling) and checked optically prior to installation in the instrument housing.

In the initial stages of the bonded configuration beamsplitter development, two major problems were encountered. First, the substrates were distorted when the mounting rings were fastened together with machine screws even though the mating surface had been polished flat to within 0.25×10^{-4} cm. Second, further distortion of the beamsplitter substrate was encountered when the assembly was subjected to environmental testing. The first problem was

resolved when the mount halves were bonded together and machine screws were used only for aligning the two mount sections. The second problem, believed to be caused by residual stresses in the beamsplitter coatings, was resolved by depositing the coatings at a controlled rate and at the same time maintaining the substrate temperature below 40 °C during the coating process.

2. Entrance window. The incoming radiation to the optical module must first pass through an entrance window located in the optical housing. This window is also used to support an optical filter which limits the short-wavelength incident infrared radiant energy. Moreover, it protects the IRIS optics from dust and humidity by partially sealing the optical cavity, which is kept under continuous nitrogen purge except when the instrument is operated in vacuum. In order to adequately pass the longer wavelengths required for IRIS-M, the entrance window material was changed from Irtran-6, used on IRIS-D, to CsI. The change of material, required that the window be protected from humidity in a manner similar to that adopted for the CsI beamsplitter.

3. Image motion compensation and calibration (IMCC). The IMCC subassembly, which consists of an elliptical mirror driven by two dc torque motors in tandem, is used to channel radiation from either the planet, the on-board warm blackbody, or outer space to the optical module. In the planet position near periapsis, the mirror also can be commanded to rotate linearly about its axis to minimize in one plane the image smear caused by spacecraft motion during the 18.2-s interferogram duration.

B. Electronics

The block diagram of the IRIS-M electronics system is shown in Fig. 3.

1. Phase-locked loop and vibration. The Michelson mirror drive system shown in Fig. 3 is a single-side-band phase-locked loop that slaves the moving mirror motion to a spacecraft clock frequency. This system, which is very similar to IRIS-D, provides, in addition to a tight velocity control for the Michelson mirror, a strobe pulse for sampling the IR detector signal output at equal intervals of mirror displacement. This pulse is synchronized in phase and frequency with the spacecraft clock. As discussed in Ref. 2, the primary effect of mechanical vibration on the

instrument is to cause a delay modulation in both the neon (reference) and infrared channels. The technique employed on IRIS-M is similar to that tested for IRIS-D, but capable of functioning under higher vibration levels. These higher vibration levels caused a higher modulation index which spread the signal spectrum over a broader frequency band. With the increased spectral resolution specified for IRIS-M, more effective suppression was necessary than that available from the IRIS-D design.

2. Vibration suppression, delay line. The system shown in Fig. 3 was used to accommodate the wider bandwidth. The initial sampling rate was increased by a factor of 3 over IRIS-D by sampling every neon fringe. However, because of the sample averaging technique performed (described in the following subsection), the resultant data output of IRIS is 3 fringes per word sample interval, the same number indicated in Table 1 for IRIS-D. The low-pass filter contained in the reference channel also had its cutoff frequency extended approximately by the same factor of 3 to allow for the passage of higher-order sidebands. The sampling signal derived from this channel was delayed by an amount equal to the data channel filter delay and was used to gate the sample-and-hold circuit that precedes the analog-to-digital converter (ADC). Phase synchronization is then restored to the quantized samples by strobing the output register with the spacecraft clock. Thus, a series of digitized samples is obtained in which the effects of vibration have been minimized. However, the system is subject to some restrictions. First, the delay modulation must not exceed a value at which the sidebands generated exceed the bandwidth of the data channel filter. Second, the jitter in the reference channel produced by vibration must not exceed one-half of the period of the initial sampling frequency.

On Nimbus, the IRIS was solidly installed to the main spacecraft structure and the vibration levels were low enough so that the added complexity of the delay circuitry was deemed unnecessary. On Mariner, IRIS is mounted to the scan platform, resulting in a higher operational vibration environment. The implementation of the delay line was necessary to meet the NER performance requirements. The amount of delay is determined by the slope of the phase shift vs frequency curve of the analog infrared channel filter. The 270-Hz low-pass filter implemented is functionally identical to the filter used on IRIS-D, i.e., third-order maximal flat filter sections

cascaded with first-order all-pass phase correction networks. The resulting time delay is approximately 5 ms. An equal delay of the neon sample pulse stream is achieved by clocking the pulses through a shift register where the time interval is determined by the proper selection of a clock frequency.

3. Summation unit. The purpose of the summation unit is to provide additional filtering of the data. Since the bandwidth established (see aliasing below) for what is considered to be the worst case vibration environment is 3 times that for a quiet environment, significant noise reduction may be achieved through sample averaging. Also, since this is a wholly digital operation using the already quantized samples, no additional errors were introduced. Finally, provided that the behavior of the ADC is accurate about zero (which proved to be the case), the size of the least significant quantized bit is effectively reduced by a factor of 3, while the dynamic range is increased by the same amount. In summary, then, the digital summation unit provides a simple and accurate method of increasing the signal-to-noise ratio by a factor of $\sqrt{3}$ and extending the dynamic range by a factor of 3. This circuit has worked well in laboratory tests.

Digitization by the successive approximation method takes place at a 200-kHz rate so that a data word is available for manipulation for 1.3 ms before the next sample is taken. This time is utilized so that succeeding sets of three words are added together and the resulting 12-bit words are formatted and serially transmitted to the Mariner data handling system.

4. Quantization. General requirements placed on the ADC have been discussed in previous IRIS papers (Refs. 1 and 2). The spectral band of the Mariner instrument was extended down to 200 cm^{-1}, which increased the peak amplitude of the signal by approximately 20%. In addition, a noise equivalent radiance of 0.5×10^{-7} W cm^{-2} $ster^{-1}/cm^{-1}$ was established as a design goal. These factors resulted in a required quantization capability with at least a factor of 2 more sensitivity and a factor of 4 more range than that used for IRIS-D.

The increased sensitivity is gained by adding one step to the ADC ladder of IRIS-D. All additional circuits were of identical design to the existing stages and therefore did not require any substantial new design. The scale change was not altered and remains times 4. The digital word

produced by this conversion system is 11 bits as opposed to the 12 needed to meet the range and sensitivity stated above. The twelfth bit is produced by summing three samples together (as discussed previously).

5. Reference interferometer detector. The noise equivalent radiance (NER) of 0.5×10^{-7} W cm^{-2} $ster^{-1}/cm^{-1}$ established as a design goal for IRIS-M is the same value achieved for IRIS-D. However, an increase in spectral resolution which requires a smaller field of view and an increase in the Michelson mirror travel for IRIS M have the effect of increasing the NER, since both systems use the same type of IR detector. To compensate for some of the increase in noise, improvements were necessary in other areas. The attempt to use a pyroelectric detector, which should have resulted in an improvement over the thermistor bolometer by a factor of 2, never materialized (see Section III-B). Therefore, improvements in IRIS-M IR data electronics and sampling techniques were necessary and were achieved by the use of summation, previously described, and the implementation of the photomultiplier tube (PMT) in lieu of the photodiode used in the Nimbus IRIS for the neon detector. The IRIS-M longer Michelson mirror travel distance required that the neon detector mask size be reduced to 0.3 mm in diameter so that the signal detected would be restricted to that of a single fringe. The resulting low signal level necessitated the application of the PMT and ancillary high-voltage regulator which improved the neon amplitude modulation and subsequently increased both the IR signal-to-noise ratio and the reliability of maintaining phase lock over the testing temperature range.

C. Science Data Format

1. Housekeeping (HK) telemetry. The HK telemetry channels are included with the science IR data as in IRIS-D except for the addition of the support base temperature, neon sample delay line override indication, and IMCC mirror scan status. The IMCC mirror position indication on Nimbus was implied by command from the programmer, whereas, for Mariner, this function is definite, since it is controlled by the actuation of a reed switch at each of the three port positions.

2. IR data. As described previously, all of the 12 digital bits in each IR data word are used in the quantization process. Word synchronization for ground station acquisition is not necessary as in the case for

Nimbus (2 sync bits per word were used) since this function is provided by the spacecraft data automation subsystem (DAS).

3. Bit error detection/correction. The IRIS-D instrument requirements specified that the science data stored by the Nimbus spacecraft recorder and played back at 120 kbits/s shall have a bit error better than 10^{-5}. This has been achieved by Nimbus 4 throughout at least 17 months of operation. For the Mariner mission, however, the 8.1-kbits/s real-time science telecommunication channel is expected to have a bit error of 10^{-3} for a worst case about midway into the mission (Fig. 4). Therefore, in order to recover the IRIS science data with a higher level of confidence, a concatenation (coding of a coded signal) scheme of the biorthoganal code with a generalized Hamming code was implemented (Ref. 4). Furthermore, the application of the technique is contained totally within the IRIS electronics, eliminating any additional burden to the spacecraft data handling system. Owing to the characteristic form of the IRIS interferograms (Fig. 5), high data confidence is attainable by just applying the parity detection and correction to the central 512 data words. Coding is not required for the remaining interferogram words in the two side portions because errors are more easily detected and corrected by the ground computer before the Fourier transformation is performed. The column and Hamming parity bits generated during the coding process to satisfy the parity equations are stored in the IRIS instrument MOSFETS register. The parity bits are then successively stripped out of the register after the second group of housekeeping data that follows the IR science data. In this manner, the biorthogonal block coded data performed by the spacecraft flight telemetry subsystem (FTS) does not include both IR data and parity bits in the same block. The FTS codes 6 bits of data into a 32-bit word, which is then transmitted to earth. The IRIS parity design also satisfies the requirements that the addition of the parity generator will not disturb the IRIS data format and any failure in the encoder will not affect the science data. Figure 6 shows the probability of bit error for the biorthogonal code without the IRIS parity detection and correction system and a comparison of the Mariner system and the concatenated code assuming error correction for nonsynchronous and synchronous cases. The synchronization refers to the phasing of IRIS words into the block coding. Although the synchronized system would decrease the bit error by a factor of 10, the nonsynchronous system was implemented

because of its simplicity and because it does not require any modifications to the spacecraft FTS.

D. Thermal Control

1. Optical module. The radiometric calibration and optical alignment of the IRIS system depend on the stability of the optics housing temperature. Therefore, an active thermal control system is employed to stabilize the interferometer housing temperature at 248 ±0.2°K. Instrument power is dissipated by a shaded radiator which is an integral part of the optics housing. The radiative surface is coated with white paint having a low value of solar absorptivity/IR emissivity (α_s/ϵ). The radiator shade is lined with an aluminized reflector to increase the effective view factor to deep space. A second deployable shade is used to reduce the amount of planetary flux which is absorbed by the radiator during the periapsis pass. This shade reduces the transient radiant load from a peak of 8 W to a peak of about 3 W. All exterior surfaces of the interferometer except the radiator and the viewing ports are covered with superinsulation blankets.

Thermal control of the IRIS sensor is achieved by designing the radiator to have excess radiative power and providing a thermostatic heater which supplements the internally dissipated electronics power of the instrument as required for thermal stability. Both the heaters and the temperature control sensor are bonded to the optics housing.

As shown in Fig. 7 the thermal control limits are set by the radiative power of the instrument, 17.1 W at 248°K, and the maximum heater power of 9.5 W. The width of this control region is sufficient to accommodate the following thermal factors which change during the mission:

(1) Heat conduction from support base.

(2) Solar panel radiant input.

(3) Mars radiant input at periapsis.

(4) Voltage to the control heaters.

Figure 7 illustrates the power balance as a function of orbital position during the first day of the 90-day mission. At apoapsis the thermal load to the radiator is 9.6 W. The thermostatically controlled heater supplies an additional 7.5 W to match the radiative power of the instrument at 248°K.

Near periapsis the absorbed planet radiation adds 3 W, and the heater power is reduced a corresponding amount. This control method keeps the total load to the radiator at a constant 17.1 W. The on-off thermostat trip-points are ±0.2°C; therefore, the IRIS instrument should be stabilized at 248 ±0.2°K during the entire 90-day mission.

2. Warm blackbody calibration. The temperature of the calibration blackbody mounted to IRIS support base is also stabilized with an on-off thermostat-controlled heater. A disc heater and sensor are bonded directly to the base of the blackbody. Heater power of 1.5 W is sufficient to provide a controlled blackbody temperature of 296.4 ±0.2°K over the extremes of support base temperature.

III. TEST PROGRAM

A. Subsystem Level Testing at Texas Instruments, Inc.

Three flight models of IRIS-M were fabricated and qualified for flight use:

(1) Flight 1 (SN 103)

(2) Flight 2 (SN 104)

(3) PTM/Flight Support Model (SN 105)

An engineering model (SN 102) was delivered to JPL for bench integration tests. This unit was used subsequently for electrical integration tests of subassemblies at the Texas Instruments facility. Prior to the qualification and acceptance testing of IRIS at Texas Instruments, the following subassemblies were subjected to functional and environmental tests:

(1) IR detector assembly field of view (FOV).

(2) Beamsplitter.

(3) Michelson mirror drive assembly.

(4) IMCC torque motor.

(5) Electronic subassemblies.

(6) Optical alignment.

Major electronic subassemblies were integrated and tested with a complete breadboard instrument prior to the assembly of the flight subsystem. The following qualification and flight acceptance tests were conducted at the contractor's facility.

(1) Sine and random vibration.

(2) Temperature cycling.

(3) Thermal vacuum.

B. Major Problems and Resolution

During the development and testing of the Mariner Mars 1971 IRIS, many problems in the optical, mechanical, thermal and electronic areas had to be resolved. The major problems related to the design are summarized in Table 2.

C. Subsystem Level Testing at JPL

Two tests, an acoustic vibration test and an interface test with the DAS, were done at JPL. Additionally, bench testing was done each time an instrument was returned to JPL and before delivery to the Spacecraft Assembly Facility (SAF). The engineering model IRIS (SN 102) was successfully interfaced with the DAS and power supply, and no problems resulted from the acoustic test of the PTM (SN 105). Bench checkout equipment (BCE) and the test and formatter equipment were also used in a clean room to troubleshoot problems that occurred in the SAF. Only one problem occurred during a receiving test with the BCE, namely, a failure of the Michelson motor of SN 103 to phase-lock with the neon signal of the reference interferometer. The instrument was returned to Texas Instruments, and the problem never reoccurred.

D. System Level Testing at JPL

System level testing was accomplished at three locations: the Spacecraft Assembly Facility (SAF); the JPL Environmental Test Laboratory (ETL), where acoustical vibration, radio frequency interference (RFI), and thermal-vacuum testing was done; and at the Air Force Eastern Test Range (AFETR). At AFETR, in addition to SAF-type testing at an ambient environment, tests were conducted in the Explosive Safe Facility (ESF) and on the launch pad in launch configuration. The instrument interfaced with other science subsystems and the spacecraft for the first time in the SAF. Table 3 shows the significant failures and anomalies that developed as the result of system testing. Only five problems were interface problems: (1) 2400-Hz transient coupling to the ±600-Vdc power supply (5/5/70), (2) IMCC mirror scan reversed (5/14/70), (3) miswired SOSE cable (7/23/70), (4) otpics module out of thermal control (8/6/70), and (5) capacitor failure in reverse bias (4/22/71). All the others in the table were instrument failures. The lack of thermal margin during thermal-vacuum testing led to an extensive redesign of IRIS thermal control which included the addition of a planet shade for the radiating surface. The IRIS demonstrated performance parameters approached the design goals. The major problem during system testing at AFETR was the capacitor failure in SN 104 caused by reverse bias during the standby mode.

The three instruments logged system test time as follows: SN 103, 250 h; SN 104, 196 h; and SN 105, 126 h. Total test time at JPL and at the vendor ran respectively 821, 470, and 481 h.

E. IRIS Flight Schedule

Figure 8 shows the delivery schedule for the three flight models. Table 4 describes the problems and retrofit performed at Texas Instruments, Inc. After each rework cycle the instruments were subjected to a modified FA vibration and temperature requalification test.

F. Performance

The spectral responsivity and NER (Ref. 5) for SN 105 during the thermal-vacuum flight acceptance tests are shown in Figs. 9 and 10, respectively. The plots were computed from averaging six pairs of cold (78°K) and warm (296°K) blackbody calibrations with the instrument at its specified operational temperature. The drop in responsivity at 350 cm^{-1} is caused by the absorption of the optical coatings. The NER over the passband met the design goal of 0.5×10^{-7} W cm^{-2} $ster^{-1}/cm^{-1}$. From launch (May 30, 1971), SN 105 was in the standby mode during the interplanetary cruise where only the heater control circuit is energized to maintain the optics and warm calibration blackbody at proper operating temperature. Based on the telemetry data received, the thermal control met the design requirements.

G. Synthetic Spectrum

A theoretical Martian brightness temperature spectrum, computed using a Mars model atmosphere, is shown in Fig. 11. The synthetic spectrum shown was computed utilizing the spectral resolution and NER characteristics of IRIS-M, and thus represents a typical Martian spectrum that might be obtained during the orbital mission. The model atmosphere contains approximately 30×10^{-4} cm precipitable water vapor with the water vapor absorption features being evident in the 200-400 and 1400-1600 cm^{-1} region of the spectrum. Strong CO_2 absorption is seen in the 550-750 cm^{-1} region. Martian surface effects may be studied in the Martian atmospheric "windows" at 400-500 and 800-1200 cm^{-1}.

REFERENCES

1. Hanel, R. A., et al., Appl. Opt., 9, 1967, August 1970.

2. Hanel, R. A., et al., Appl. Opt., 10, 1376, June 1971

3. Design and Development of Cesium Iodide Beamsplitter for IRIS Instruments. Engineering Report, NASA/GSFC Contract NAS 5-11620. Texas Instruments, Inc., Dallas, Texas, December 15, 1970.

4. Dorsch, B., and Miller, W. H., GSFC NASA TN D-5775, June 1970.

5. Hanel, R. A., et al., Icarus, 12, 48-62, 1970.

Table 1. Characteristic parameters of Nimbus and Mariner interferometers

Parameter	IRIS-B	IRIS-D	IRIS-M
Nominal spectral range, cm^{-1}	400 to 2000	400 to 1600	200 to 1600
Number of samples per interferogram	3408	4096	4096
Reference wavelength, cm	0.5852×10^{-4}	0.5852×10^{-4}	0.6929×10^{-4}
Number of reference fringes per sample interval	2	3	3
Optical path difference, cm	0.4	0.72	0.85
Displacement of mirror during interferogram, cm	0.2	0.36	0.427
Velocity of mirror, cm s^{-1}	0.0184	0.0275	0.0235
Width of resolved spectral intervals, apodized (unapodized), cm^{-1}	5 (2.5)	2.8 (1.4)	2.4 (1.2)
Area of aperture, cm^2	13	15	15
Solid angle, sterad	1.57×10^{-2}	5.5×10^{-3}	4.7×10^{-3}
Field of view, deg	~8	~5	~4.5
Duration of interferogram, s	10.956	13.107	18.2
Basic frame period, s	16	16	21
Bits in analog-to-digital converter	8 + gain	9 + gain	11 + gain
Neon reference frequency, Hz	625	937.5	675
Frequencies in data channel, Hz	18 to 73	11 to 88	9.5 to 75.8
Number of resolved spectral intervals, apodized	320	430	585
Noise equivalent radiance, W cm^{-2} $ster^{-1}/cm^{-1}$	0.6 to 2×10^{-7}	0.5 to 1×10^{-7}	0.5 to 1×10^{-7}
Operating temperature of detector, °K	250	250	250
Weight, kg			
Optical module	10.47	14.55	20.00
Electronic modules	4.13	7.62	3.26
Outline dimensions, cm			
Optical module	$38.9 \times 32.2 \times 21.3$	$43.9 \times 38.9 \times 27.9$	$44.2 \times 37.6 \times 34.5$
Electronic modules	$20.3 \times 15.2 \times 16.5$	$20.3 \times 15.2 \times 16.5$ $10.2 \times 15.2 \times 16.5$	$17.5 \times 15.7 \times 8.1$ $17.5 \times 15.7 \times 8.1$ $17.5 \times 15.7 \times 4.1$
Average power, W	16	28	26

Table 2. Resolution of design problems

Problem	Resolution
Maintaining optical alignment during vibration testing and temperature cycling	Redesigned fixed mirror mount and screws Increased stiffness of optical housing and Michelson mirror motor mount
Maintaining optical flatness of cesium iodide (CsI) beamsplitter during vibration and temperature cycling	Redesigned beamsplitter mount to improve support of CsI substrates Optical coatings deposited at lower and controlled temperatures
Pyroelectric IR detector mechanical and electrical integrity could not be maintained over long time duration	Supplanted with thermistor bolometer (used on Nimbus IRIS)
IMCC torque motor	
Shaft failed during vibration qualification	Redesigned shaft back to IRIS-D configuration
Shaft binding during thermal vacuum and cold alignment testing	Changed coil potting material Added mounting screws
Spacecraft 2.4-KHz power turn-on transient too large	High-voltage input removed from surge limiter and reactance added to high-voltage line
Spacecraft 2.4-KHz power supply variations affected neon reference signal, which caused loss of phase lock	Added a ±600-V regulator for photomultiplier tube
Michelson motor phase-locked loop instability at low temperatures caused 6.3-KHz modulation of neon reference signal	Reduced open-loop gain of velocity feedback loop
Reverse bias voltage on wet slug tantalum capacitors when primary power off and standby power on	Added transistor switches to IMCC circuit to isolate leakage current Supplanted some capacitors with dry type tantalum
Optical module thermal control/ margin	Resolved spacecraft and IRIS interfaces Increased radiative surface and heater power Added deployable shade to reduce planetary heat flux

Table 3. Significant test failures and anomalies (system level)

Date	S/C	Environment	Location	Description
	Engineering Model (S/N 102)			
5/5/70	71-3	Ambient	SAF	Transcients on the S/C 2400 Hz power were being coupled through the IRIS ± 600 vdc power supply.
5/14/70	"	"	"	IMCC mirror scan direction was reversed. The direction was left as used on IRIS B&D.
5/19/70	"	"	"	Warm blackbody heater was locked up in the on state. Failure caused by accidental voltage application.
5/27/70	"	"	"	Miswired connectors on ± 600 vdc reg.
"	"	"	"	Parity generator failed, due to a reverse voltage. Design error.
6/10/70	"	"	"	Third MSB of IRIS data words locked up in "1" state; broken wire in the IRIS parity box.
	Flight 1 (S/N 103)			
7/23/70	"	"	ETL	Parity generator failed, diode added to prevent reverse voltage.
"	"	"	"	Miswired direct access cable shorted IRIS supply voltages together & caused overstress of numerous components.
8/6/70	"	ther/vac	"	IRIS optics cube went out of thermal control. Extensive thermal redesign was required on all IRIS instruments.
	Flight 2 (S/N 104)			
9/23/70	71-1	"	SAF	IRIS drew twice its normal power. A polarized capacitor was installed backwards in Bolo, Reg.
4/22/71	"	launch pad	ETR	IRIS failed at IRIS power on. Low reverse bias on polarized capacitors caused the failure. Redesign was required on all IRIS instruments.
	PTM/SM (S/N 105)			
1/15/71	71-2	ther/vac	ETL	High rate data failed during ther/vac. No discrete failure found at TI. The parity box was removed, but checked OK. After it was replaced, the failure was not present.

Table 4. Flight model retrofit schedule

Retrofit Designation (Figure 8)	Retrofit/Problem
S/N 103	
A	• Replaced overstressed components (SOSE cable short); thermal mods.
B	• Phase lock loop (PLL) failed during B.T. at JPL (not resolved at T.I.).
C	• Reduced bolometer preamp capacitor to improve IR frequency response to step target temperature. PLL zener diodes replaced. Reduced open loop gain of Michelson motor vel. loop at resonant frequency because of 6.2 KHz modulation of neon signal. Fixed mirror screws & washers replaced. Replaced Nimbus-D IMCC torque motor with Mariner motor S/N 70E906.
K	• Returned to T.I. because of capacitor problem on S/N 104 (replaced 37 capacitors)
	• Added 100 pf capacitor to the input of the bolometer preamplifier to prevent the amplifier from oscillating at 250°K.
	• Added redundant chassis ground in the data box to existing common signal/ power ground lead.
S/N 104	
D	• Replaced over-stressed components because of rev. polar.capacitor in bolo reg.
	• PLL anomaly, intermittent, some rework but did not replace diodes.
	• Replaced failed 2N5093 in PMT reg after wk. vibr. test.
	• Installed S/N 105 bolo. bias reg. because S/N 104 reg. was noisy.

Table 4 (contd)

Retrofit Designation (Figure 8)	Retrofit/Problem
E	• Returned to T.I. to investigate 6.2 KHz neon modulation. Reduction of vel loop gain was first accomplished on this instrument.
	• PLL failed at T.I. during B.T. - shorted IN752A zener - replaced 4 diodes.
	• Reduced bolo preamp capacitor.
	• Replaced fixed mirror screws & washers.
H	• Returned to T.I. to investigate failure during spacecraft 1 tests. Decoupling wet slug tantalum capacitor (100μF) on H.K. multiplexer board was shorted. Investigation proved that in standby mode (cruise) 0.850 volts reverse bias on +12 volt line. Replaced 36 capacitors, bolometer decoupling capacity wasn't replaced.
S/N 105	
F	• During this retrofit cycle the PTM was rebuilt & qualified for a flight instr. (bolo. capacitor changed).
G	• Returned to T.I. because of digitizing failure (intermittent) at JPL, replaced 28 components because failure was never resolved. Incorporated diode (PLL), fixed mirror & 6.2 KHz noise on neon changes.
I	• Returned to T.I. because of capacitor problem on S/N 104. (Replaced 37 capacitors).

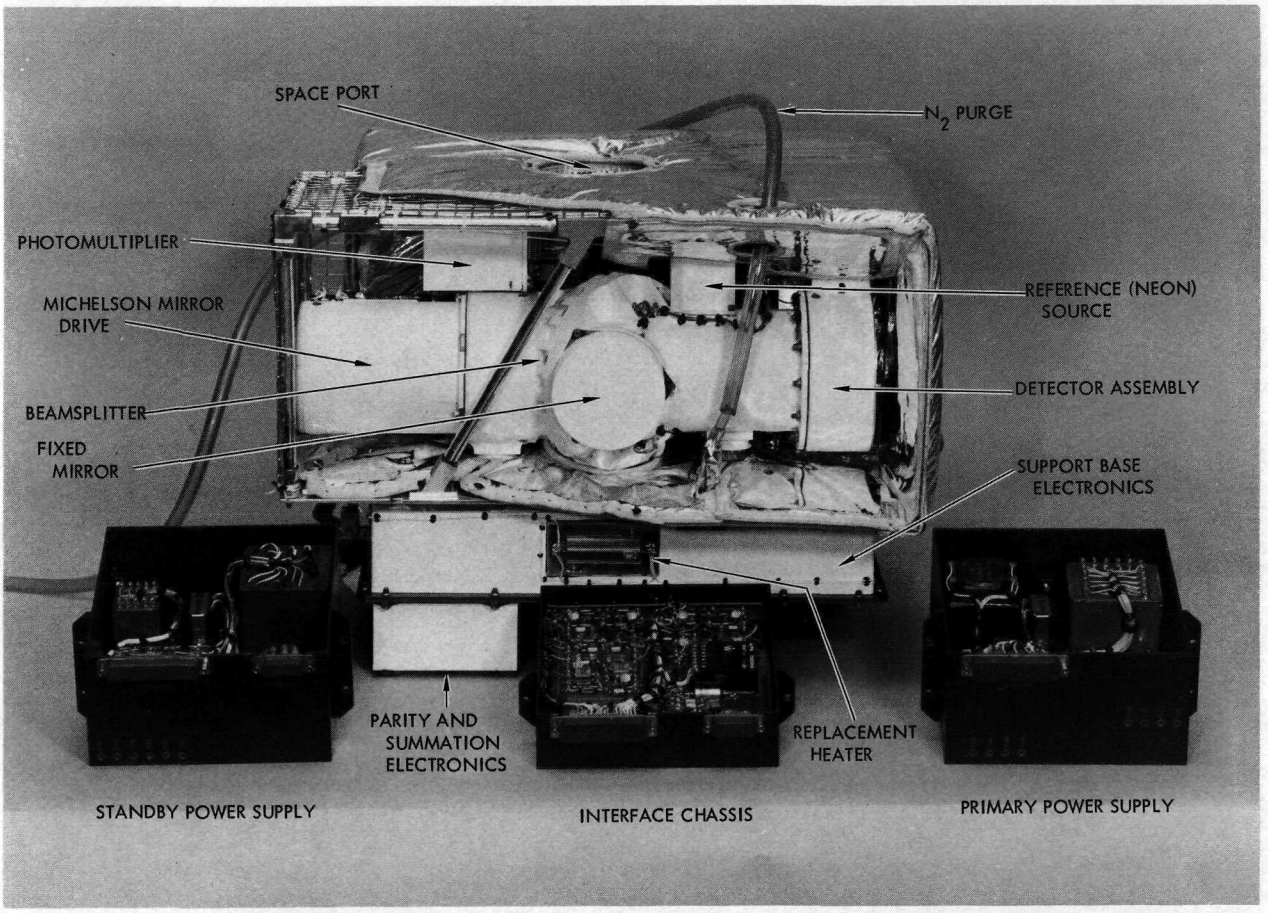

Fig. 1. Infrared interferometer spectrometer (IRIS)

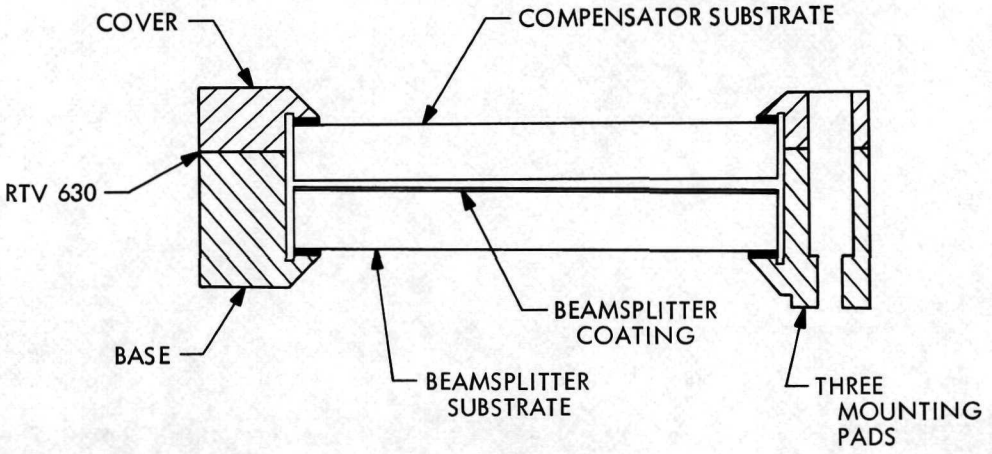

Fig. 2. Sectional view of cylindrical CsI beamsplitter assembly

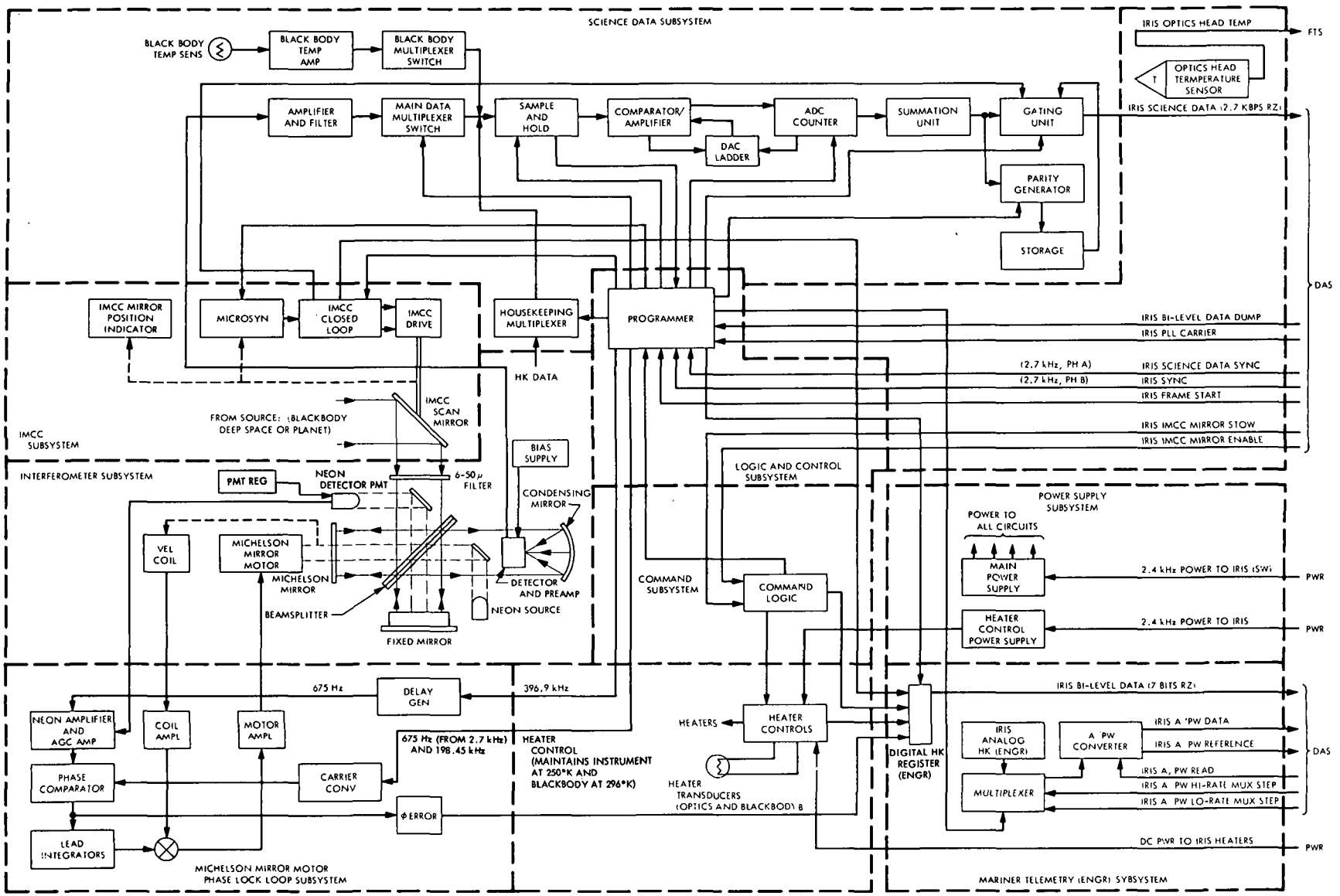

Fig. 3. Mariner Mars 1971 IRIS block diagram

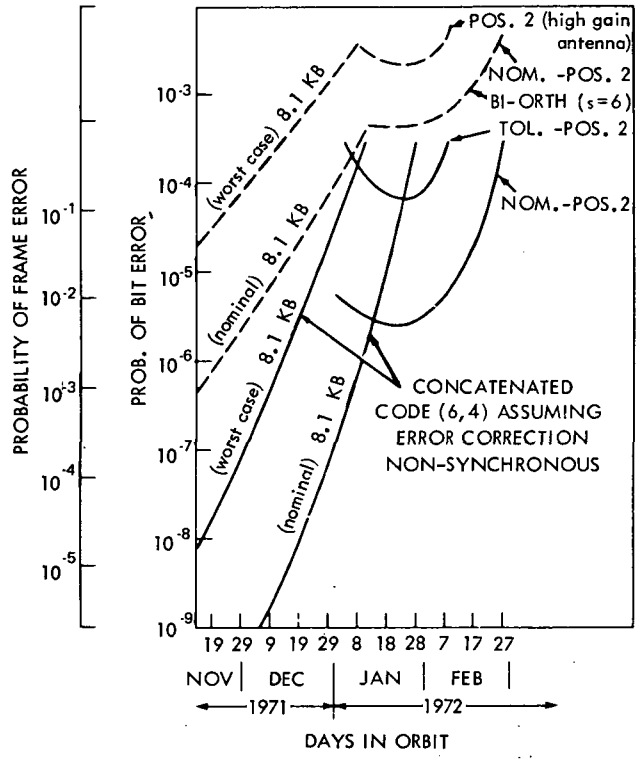

Fig. 4. Comparison of coding techniques for Martian orbit

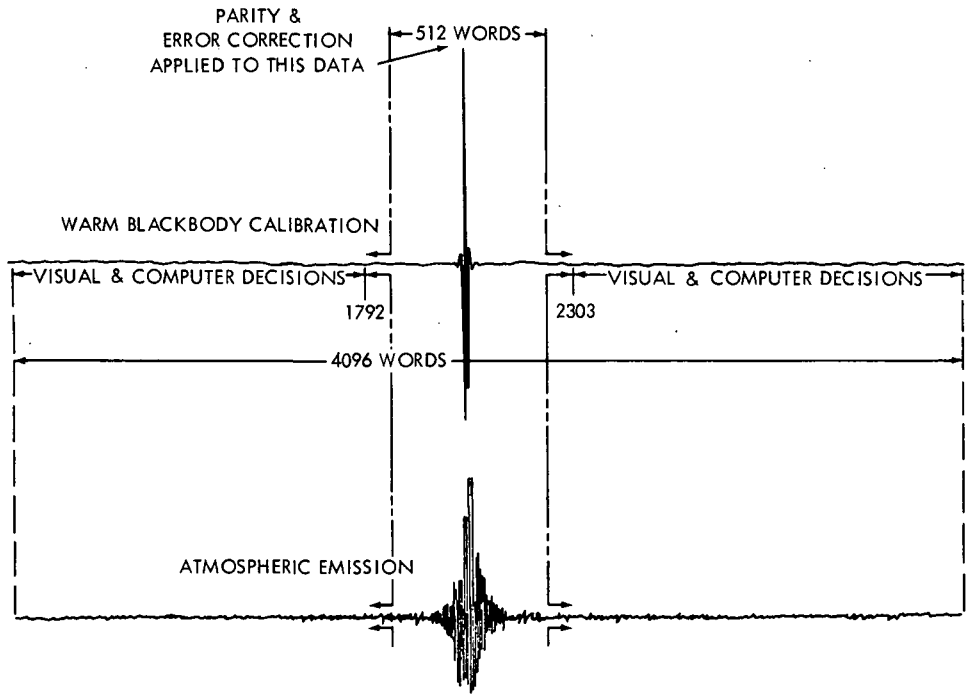

Fig. 5. Method of applying error correction to IRIS interferograms

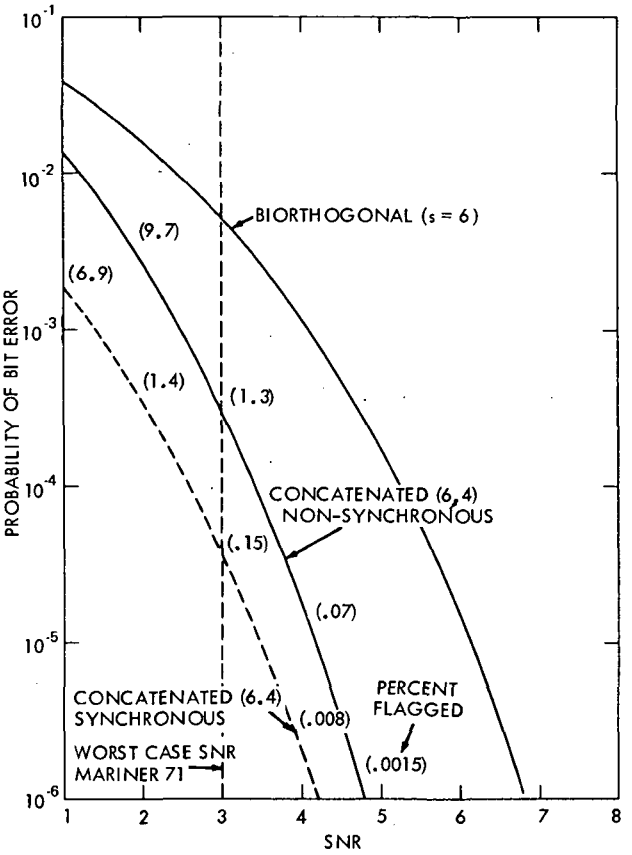

Fig. 6. Probability of bit error after correction vs SNR for concatenated (6, 4) synchronous and nonsynchronous systems as referenced to a biorthogonal (S = 6) code

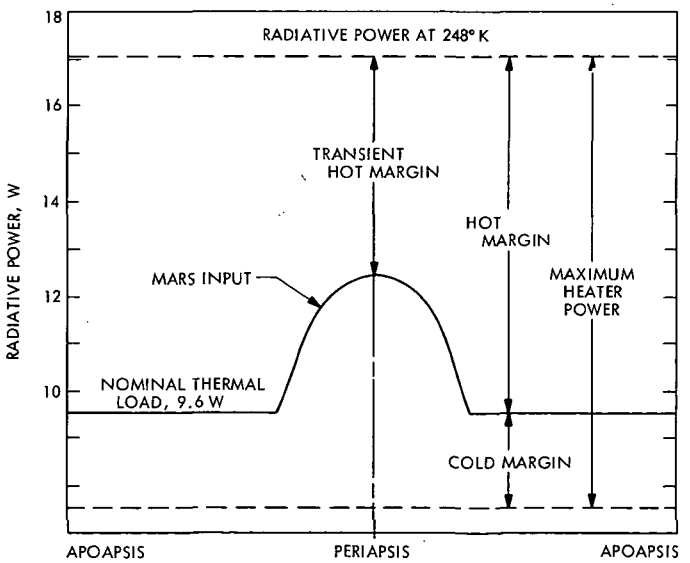

Fig. 7. IRIS thermal control, primary power on Day 0

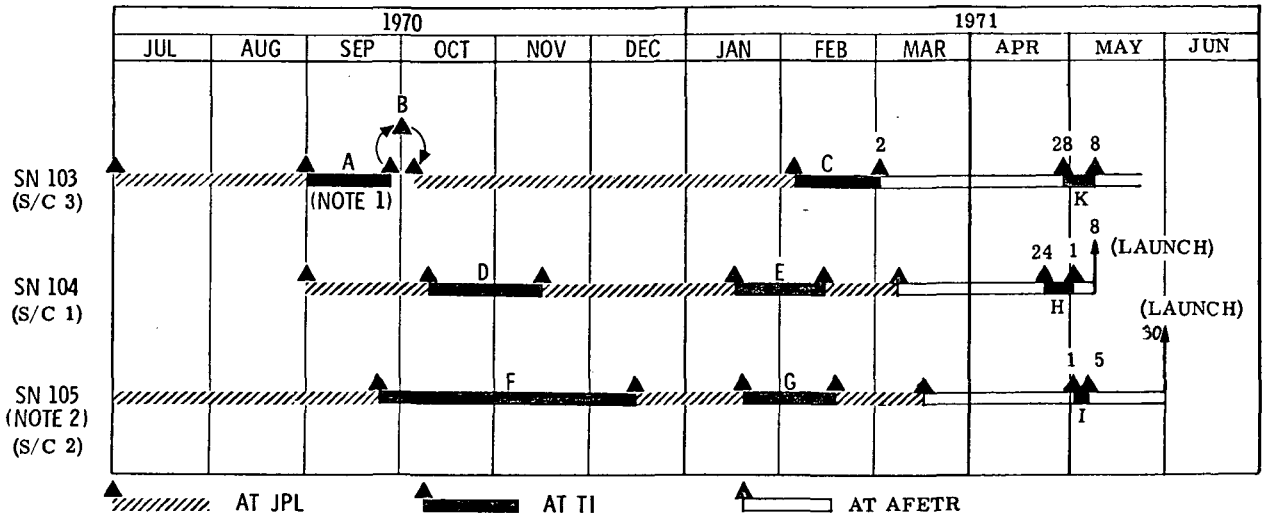

NOTES:

1. LETTERS DESIGNATE RETROFIT EFFORT AT TI
2. THIS INSTRUMENT RESULTED FROM RETROFIT OF PTM (9-26-70)

Fig. 8. IRIS milestone flight model schedule

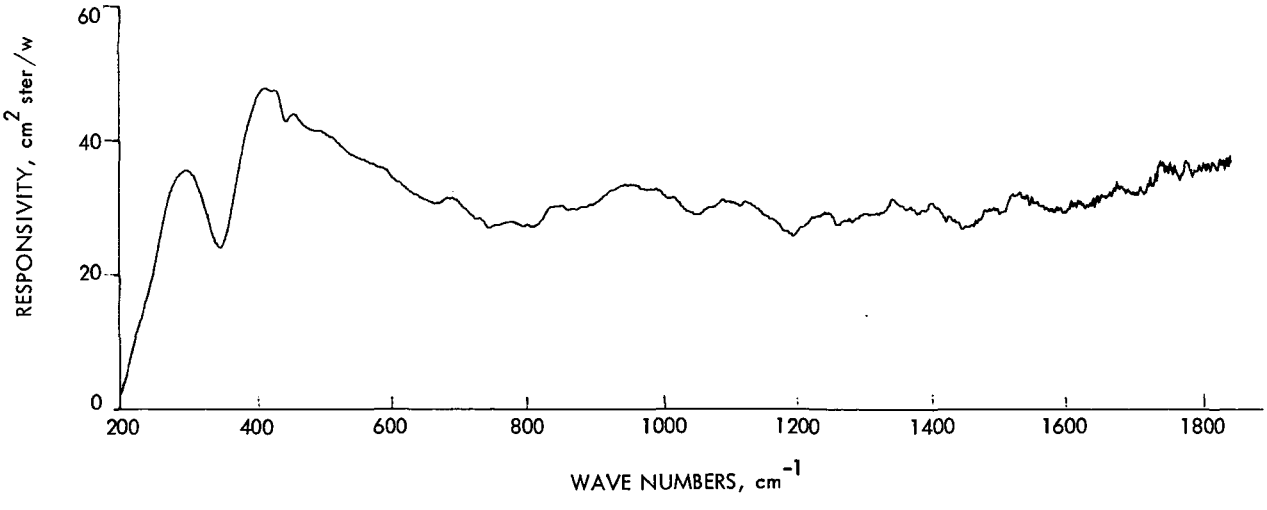

Fig. 9. Responsivity of SN 105 during thermal/vacuum flight acceptance test

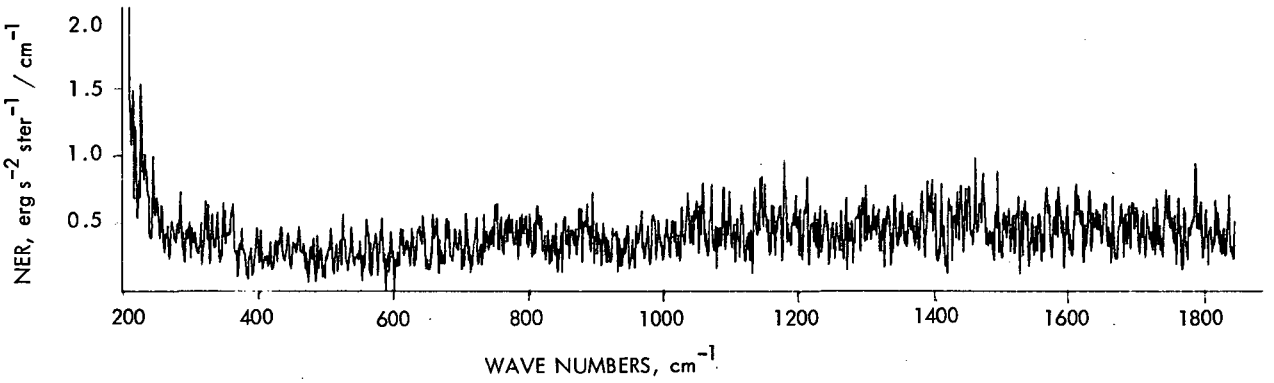

Fig. 10. Noise equivalent radiance (NER) of SN 105 during thermal/vacuum flight

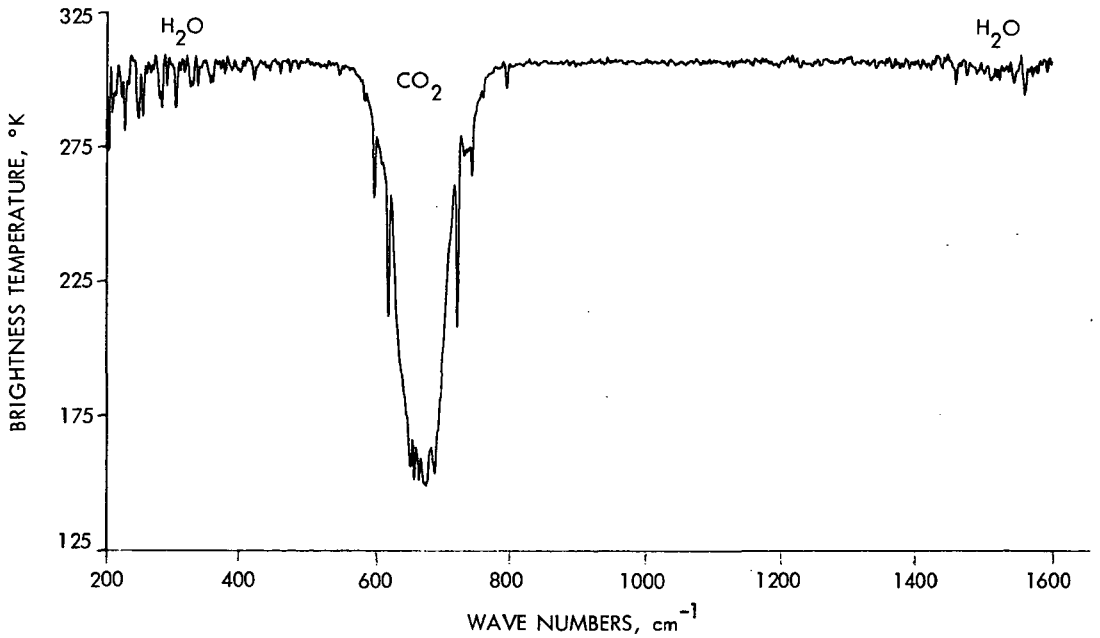

Fig. 11. Synthetic spectrum

NASA — JPL — Coml., L.A., Calif.